Carbon in the Universe

Th. Henning and F. Salama

Carbon is a major player in the evolutionary scheme of the universe because of its abundance and its ability to form complex species. It is also a key element in the evolution of prebiotic molecules. The different forms of cosmic carbon are reviewed ranging from carbon atoms and carbon-bearing molecules to complex, solid-state, carbonaceous structures. The current state of knowledge is assessed on the observational and laboratory fronts. Fundamental astrophysical implications are examined as well as the impact of these studies on the hitherto poorly understood physical and chemical properties of carbon materials in space.

More than 75% of the 118 interstellar and circumstellar molecules identified to date (*1*) are C-bearing molecules, and one component of interstellar (IS) dust is carbonaceous. The cosmic evolution of C from the interstellar medium (ISM) into protoplanetary disks and planetesimals, and finally onto habitable bodies is intrinsic to the study of the origin of life.

Carbon plays an important role in the physical evolution of the ISM because it is the main supplier of free electrons in diffuse IS clouds, thus contributing to the heating of IS gas. Emission lines of neutral (CI) (*2*) and ionized (CII and CIV) atomic C are important cooling channels for the warm IS gas and are used to probe its density and temperature. Similarly, the rotational transitions of CO, which are collisionally excited by H_2, constitute an important tracer of molecular gas in the universe.

The observation of unidentified, ubiquitous, molecular and solid-state features in astronomical spectra and the realization that these features are linked to carbonaceous materials have resulted in major scientific progress in the last 10 years. Laboratory and theoretical studies stimulated by these astronomical observations have led to a better understanding of the various forms of cosmic C such as polycyclic aromatic hydrocarbons (PAHs), C-chain molecules, C clusters, and carbonaceous solids. Ultimately, these astrophysically motivated investigations have led to the detection of novel forms of C and laid the foundations for the chemistry of fullerenes. We review the different forms of C in space ranging from C atoms and C-bearing molecules to complex, solid-state structures and discuss their importance in understanding the physical nature of the universe and its evolution.

Nucleosynthesis and Cosmic Abundance of Carbon

Carbon is the first of the lighter elements that is exclusively formed in the interiors of stars. After the proton-proton or CNO hydrogen-burning phase in the stellar core has ceased, the central temperature and pressure in stars with masses $M \geq 0.5\ M_\odot$ rise to values at which He is ignited (*3*). In these stars the central He core contracts and the outer layers expand and cool. The objects become red giants.

The 3α process (*4*) bridges the gap between the nuclei masses 4 (helium) and 12 (carbon) (*5*). The resonant formation of ^{12}C, added to its inefficient (nonresonant) transformation into ^{16}O, forms the combination that is responsible for the presence of C in the universe.

Asymptotic giant branch (AGB) stars (*6*) are important contributors to the chemical evolution of the ISM. Dredge-up processes driven by convection in the outer layers of the AGB stars transport elemental C and O from their C-O cores to their surfaces. Oxygen-rich or C-rich molecules and refractory solids may form in the extended envelopes around these stars depending on the chemical and physical conditions, and in particular on the C/O ratio. The less abundant element is often locked up in the stable CO molecule (*7*). Mass loss rates of AGB stars are high, between 10^{-5} and $10^{-7}\ M_\odot\ \mathrm{year}^{-1}$. Giants provide the largest contribution to the stardust injection into the ISM with a value of about $5 \times 10^{-6}\ M_\odot\ \mathrm{kpc}^{-2}\ \mathrm{year}^{-1}$ (*8*). The total production rate of solid C from C-rich stars (*9*) is about $0.002\ M_\odot\ \mathrm{year}^{-1}$.

The amount of C available for the formation of carbonaceous solids and complex C molecules is determined by the difference between the standard (the cosmic) total abundance of C relative to H $[C/H]^c$ in the local ISM and its abundance in the gas phase $[C/H]^g$. In the past, the cosmic abundance value for the local ISM was generally identified with the solar value, $(355 \pm 43) \times 10^{-6}$ (*10*), implicitly assuming a well-mixed state of the ISM and no further evolution of the total elemental abundances since the formation of the solar system 4.6×10^9 years ago. A detailed analysis of CNO abundances in B stars and HII regions (*11*)—which should reflect the present ISM values—together with the analysis of O and Kr data suggests a reduction of the cosmic abundance to about two-thirds of the solar abundance for these elements (*12*, *13*). This would imply a $[C/H]^c$ value of 237×10^{-6} with a recommended IS abundance of $(225 \pm 50) \times 10^{-6}$ (*12*). Absorption line spectroscopy in the weak CII intersystem transition at 232.5 nm with the Goddard high-resolution spectrograph (GHRS) on board the Hubble space telescope (HST) yielded $[C/H]^g$ values between $(140 \pm 20) \times 10^{-6}$ (six different lines of sight) and $(106 \pm 38) \times 10^{-6}$ (abundance determination for a translucent cloud) (*14*). The nearly constant IS gas-phase C/H ratio over a wide range of fractional H_2 abundances suggests that there is no strong net exchange of C between the gas and dust phases of the diffuse ISM. Furthermore, the C/H abundance pattern implies that, in diffuse IS clouds, solid C can only exist in grains that cannot be vaporized by shock waves. These observations suggest that either 215-C atoms (solar value) or 85-C atoms ("cosmic" value) per 10^6 hydrogen nuclei are available for carbonaceous dust particles and C-containing molecules. The latest composite and core/mantle dust models based on realistic optical constants require between 150 and 200 C atoms per 10^6 hydrogen nuclei to be in dust grains.

Atomic Carbon

Spectroscopy remotely probes the atomic and molecular composition of cosmic materials along the lines of sight. The mapping of the ISM of a galaxy through the observation of absorption or emission lines (or both) leads to the determination of the structural parameters [density, temperature, elemental abundances, far–ultraviolet (FUV) radiation field, and degree of ionization] of its various phases (*15*) and, thus, to the understanding of star formation and the life cycle of the different phases of the ISM (*16*). Carbon has an ionization potential ($E_I = 11.3$ eV) below the Lyman edge, so C is almost completely ionized in space, with the exception of C in dense clouds. In the case of the photodissociation regions (PDRs) (*17*), the absorption of FUV photons by gas and dust grains on the surface

Th. Henning is at the Astrophysikalisches Institut und Universitäts-Sternwarte, Schillergäßchen 2-3, D-07745 Jena, Germany. F. Salama is at NASA Ames Research Center Space Science Division, Moffet Field, CA 94035–1000, USA.

of molecular clouds and throughout the diffuse neutral ISM leads to the intense $^2P_{3/2}$–$^2P_{1/2}$ emission of CII at 157.74 μm. This bright line of CII is an important cooling channel in moderate- and low-density regions of the ISM and is used to map the galaxy (*18*). Deeper in the PDRs, CI 370 ($^3P_2$–$^3P_1$) and 609 ($^3P_1$–$^3P_0$) μm emission lines and CO (J=1-0) rotational lines are observed (*18*). CI is dominantly formed through the photodissociation of CO. Hence, CI traces the molecular abundance in translucent clouds and samples the transition between atomic and molecular C-containing species in the ISM (*19*). The detection of radio recombination lines (C92α, C110α, C166α) arising from CII also provides information on the physical conditions (electron temperatures and electron densities) in PDRs (*20*).

CIV is detected in emission at 154.8 and 155.1 nm along several lines of sight in the ISM (*21*). The upper limits that have been placed to the CII (103.7 nm) and CIII (97.7 nm) lines constrain the parameters of the low-density, hot phase of the ISM (*21*). The absorption lines of neutral and ionized atomic C occur in the UV at wavelengths <320 nm, and their detection requires space-borne instruments. GHRS has detected the absorption lines associated with CI and CII in cool neutral gas and with CIV in the hot ISM. CII is the dominant state of C in diffuse clouds and is detected through its strong resonant line at 133.5 nm and in its weak intersystem transition ($^2P_{1/2}$–$^4P_{1/2}$) at 232.5 nm. CI is detected through multiplets in the 115 to120 nm range, 127 to 129 nm range, and near 132.9 nm, all originating from its ground state $2p^2\ ^3P_{0,\,1,\,2}$ (*22*). Narrow absorption components of CIV have also been detected in HII regions.

Molecular Carbon

Electronic, rotational, and vibrational spectroscopy have been used to detect various C molecules including ions and radicals, to measure their elemental abundance, and to determine the structure of C-bearing molecules in space (*23*).

The ability of C to form hybridized orbitals accounts for its rich chemistry (Table 1). Polyaromatic molecules represent the most stable configuration because all the π electrons are entirely delocalized over the molecule (*24*) (Fig. 1). The organic molecular species detected in space range from simple diatomic (for example CO, CN, C_2, CH, CH^+, CN^+, and CO^+), to simple polyatomic (CH_2, CH_4, C_2H_2, CH_3OH, CH_3CH_2OH, H_2CO, and HCN), to large, complex, unsaturated [acetylenic radicals C_nH, cyanopolyynes HC_nN, carbynes and C chains of the type C_nH_m (where $n \ll m$)] and polycyclic aromatic hydrocarbon molecules (PAHs).

The discrete absorption and emission bands observed in space act as heating and cooling lines, respectively, for the surrounding medium. Some of the molecular bands are assigned to transitions within specific molecular carriers (*25*). For example, the ubiquitous 2.6-mm line associated with the J=1-0 rotational transition of CO serves as a diagnostic for density and temperature in molecular clouds. The electronic transitions of ^{12}CO and ^{13}CO, seen in absorption near 150 and 108 nm, respectively, and corresponding to transitions to the lower excited electronic states, provide a diagnostic for density and temperature in diffuse IS clouds. Electronic transitions of CN and CH, seen in absorption at 388.3 and 432.3 nm, respectively, are used to measure the C and N abundances in the line of sight and provide a diagnostic for the fractional ionization in the clouds. The C_2 absorptions detected at 134.2 and 231.3 nm provide a diagnostic for the density and the radiation field. The strong C_2 emission bands detected in the 516.5 to 513.2 nm range (Swan system) in cometary spectra represent a sensitive probe of the rotational temperature achieved in the coma at various heliocentric distances.

Complex chemical networks have been developed to describe the formation of molecules and ions in different regions of space according to the varying physical conditions (*18*, *25*). The chemical regimes involved in the models include a combination of ion-molecule gas-phase chemistry and dust-grain surface chemistry. Shock-induced chemistry is invoked in the regions of star formation. Ion-molecule chemistry occurs through two-body collisions and is initiated by photoionization and photodissociation in diffuse clouds and by ionization by cosmic rays in dense clouds. Thus, the chemical network describing the formation of simple C molecules in diffuse clouds, where C is mostly ionized, begins with the radiative association reaction of C^+ with H_2. The resulting CH_2^+ reacts with H_2 to form CH_3^+, which produces CH and CH_2 through dissociative recombination with electrons. The reaction of these neutral molecules with C^+ leads to the formation and build-up of polyatomic hydrocarbons. This reactional scheme is limited, however, by the photodissociation of the neutral molecules at short and moderate depths and by the lockup of C in the stable CO molecule at greater depths in the cloud. In dense clouds shielded from UV radiation, C is mostly neutral and the C chemistry starts with the reaction of C with H_3^+ and the formation of CH_3^+ by the formation of CH^+ and CH_2^+.

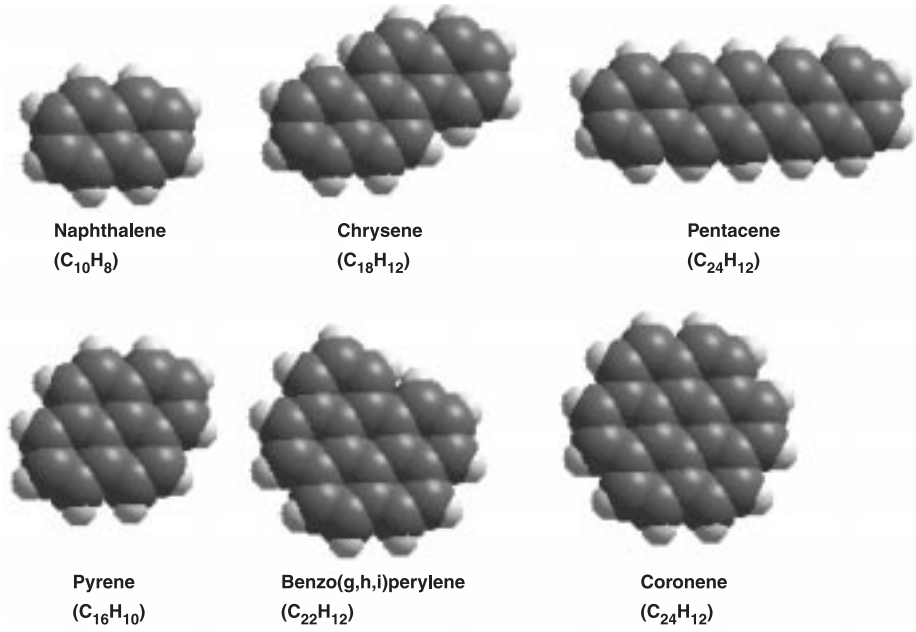

Fig. 1. Some representative PAH molecules.

Table 1. Carbon hybrid orbitals.

Atomic orbitals	Resulting hybrid orbitals	Example
$2s$, $2p_{x,y,z}$	Four equivalent sp^3 tetrahedral orbitals	Alkanes, as in CH_4
$2s$, $2p_{x,y}$, $2p_z$	Three planar sp^2 orbitals and one perpendicular p orbital ($2p_z$)	Alkenes, as in C_2H_4
$2s$, $2p_x$, $2p_{y,z}$	Two linear sp orbitals and two perpendicular p orbitals ($2p_{y,z}$)	Alkynes, as in C_2H_2

Complex hydrocarbons (such as CH_2CO, CH_3CN, and C_nH_m) are subsequently produced through C insertion reactions, condensation reactions, and radiative association reactions.

In addition to the large number of stellar and IS absorption and emission features that are associated with specific molecular carriers, a set of ubiquitous features remains unidentified in IS spectra. These features may represent a tracer for complex, C-bearing molecules in the ISM. The unidentified features are as follows: (i) A set of ubiquitous, weak, diffuse IS absorption bands (DIBs) ranging from the near ultraviolet to the near infrared (NIR) and superposed to the galactic extinction curve. The DIBs number near 200 bands and have their origin in the diffuse ISM (*26*). (ii) A set of discrete visible-emission bands (RRBs) observed in a biconical nebulae, the Red Rectangle, and in the spectrum of the hydrogen-deficient star R Coronae Borealis (*27*). The RRBs are unambiguously related to some DIBs, indicating that they originate from the same molecular carriers. (iii) A set of ubiquitous, discrete, IR emission bands, the unidentified IR bands (UIR) observed in a variety of widely contrasted IS environments (including starburst galaxies, HII regions, planetary and reflection nebulae, and the galactic diffuse ISM) (*28*). These bands are a feature of IS material illuminated by photons in the FUV-to-NIR range. Furthermore, the UIR bands are characteristic of aromatic hydrocarbon materials (*29*). The current proposed assignments for all these unidentified features involve transitions in gas-phase C-containing molecules and ions (Table 2).

PAHs are thought to be responsible for the UIR bands in the ISM and represent the most abundant class of complex molecules in space, with a relative abundance to H on the order of 10^{-7} (*29*, *30*). PAHs and unsaturated hydrocarbon chains may be the sources of the DIBs and some RRBs (*31*–*33*). PAHs consist solely of fused six-membered benzenoid rings of sp^2-hybridized C atoms and the requisite number of H atoms attached to the periphery of the molecule (Fig. 1). The resulting delocalized π electrons over the C skeleton lead to the high photostability of these molecules and to their survival in the harsh IS environment (*34*). The global IS distribution of PAHs includes neutrals and ions as well as derivatives (dehydrogenated and hydrogenated PAHs, and PAHs with substituent on the periphery) (*29*, *35*). PAHs are thought to be formed in the outflows from C-rich giant stars in a process analogous to soot formation in combustion processes (*36*). PAHs are the building blocks of soot particles and the link between molecular C in the gas phase and dust grains (or carbonaceous solids). They can also be formed from the fragmentation of C dust particles in shocked regions and from photosputtering in diffuse IS clouds (*37*). PAHs are expected to play an important role in the heating of IS gas through the supply of free electrons produced by the photoelectric effect (*18*, *38*).

Carbon chains are unsaturated hydrocarbons of the type C_nH_m (where $n \ll m$). Carbon-chain molecules may be formed in the outflows from C-rich giant stars through a combination of C^+ insertion and photocleavage (*39*). The chain size is calculated to average between 20 to 30 C atoms. Carbon chains are polar and detectable in the radio region of the spectrum. These two classes of molecules—PAHs and chains—are now thought to be common constituents of IS clouds, "hot" (100 to 200 K) molecular cloud cores, and circumstellar envelopes of C stars.

The need for a better understanding of the spectral properties of these complex molecules and ions and the role they play in the evolution of the galaxy has led to a series of laboratory studies during the past decade (*31*, *40*). The astrophysically motivated laboratory effort has resulted in progress in our understanding of the molecular spectroscopy of complex C molecules and ions, as evidenced by the discovery of fullerenes (*41*).

Laboratory astrophysics provides a realistic simulation of the conditions that exist in a given cosmic environment and provides quantitative data that are relevant to the interpretation of space observations. Low-temperature molecular spectroscopy is used to simulate environments ranging from the low-density, gaseous, diffuse ISM to the icy surfaces of IS dust grains (*31*, *40*). Matrix isolation spectroscopy (MIS) has been useful for studying molecules relevant for the ISM because the neutral and ionized molecules are fully isolated at low temperature (<5 K) in a low-polarizability medium (typically neon or argon) so that the perturbations induced in the spectrum of the trapped molecules and ions are minimized (*42*).

Laboratory experiments have shown (*31*, *40*) that (i) free, neutral PAHs have strong UV absorption bands and could contribute to the UV IS extinction curve as well as to the FUV rise (Figs. 2 and 4); (ii) when ionized, PAHs also absorb in the visible and NIR (Fig. 2) close to the position of well-known DIBs; (iii) ionized PAHs fluoresce and could contribute to the RRBs; and (iv) the IR spectra of a distribution of PAHs (neutrals and ions) provide a good fit to the UIR bands.

MIS laboratory measurements of mass-selected C_nH_m anions isolated in neon matrices have shown that C chains also absorb in the wavelength range where DIBs are found and that their strongest absorption bands shift from the blue toward the red with increasing chain length (*43*). The same experiments have also shown that C chains trapped in Ne matrices are photodissociated when exposed to photons carrying more than 6-eV energy. Carbon chains are thus not expected to be photostable under the IS radiation field. This may explain why larger chains have not been observed in the ISM (*44*).

Solid Carbon and Carbides

The analysis of the IS extinction and polarization curves at UV, optical, and NIR wavelengths and of thermal IR and submillimeter and millimeter radiation indicates that cosmic dust particles have sizes in the nanometer-to-micrometer range with the probable presence of much larger particles in protoplanetary disks. Dust spectroscopy along different lines of sight, including the diffuse ISM, molecular clouds, and circumstellar envelopes around evolved stars, is used to determine the chemical composition of the grains (*45*). The features generally attributed to carbonaceous solids are (i) a strong UV absorption band at 217.5 nm in galactic extinction curves (*46*); (ii) a UV absorption band at 240 to 250 nm in the spectra of H-deficient objects such as the R Coronae Borealis stars (*47*, *48*); (iii) the so-called "extended red emission" peaking at wavelengths between 650 and 700 nm in the spectra of reflection nebula, HII regions, planetary nebulae, and the diffuse ISM (*49*); (iv) a broad emission plateau between 6 and 9 μm in the spectra of a number of objects, including the Orion Bar and post-AGB stars (*50*); and (v) a 3.4-μm absorption feature typical for lines of sight probing the diffuse ISM and mainly present in the spectra of galactic center sources and the heavily obscured "hypergiant" Cyg OB2 No.12 (*51*) (Table 3).

In addition, a broad feature between 11.0 and 11.5 μm observed in the spectra of C-rich

Table 2. Unidentified spectral signatures attributed to gas-phase molecular C.

Feature	Proposed identification
Weak, diffuse absorption bands (DIBs) in the 400- to 1200-nm range	Electronic π-π^* transitions in neutral and ionized PAHs and unsaturated hydrocarbons
Emission bands in the Red Rectangle (RRBs) in the 500- to 700-nm range	Electronic fluorescence transitions in neutral linear C molecules (carbynes) or ionized PAHs (excitation by UV photons)
Emission bands (UIRs) around 3 μm and in the 6- to 17-μm range	Vibrational transitions in neutral and ionized PAHs (excitation by UV-NIR photons)

stars and planetary nebulae has been attributed to SiC particles (*52*). The fact that no SiC absorption features are detected in the diffuse ISM limits the amount of Si locked up in pure IS SiC grains to <5%.

"Primitive" (unaltered) chondritic meteorites contain two types of pre-solar C grains: nanodiamonds and graphitic particles (*53*). Nanodiamonds constitute the most abundant fraction with typical sizes of about 2 nm, which corresponds to a few 100 C atoms. Graphitic particles have sizes of 1 to 20 μm and contain isotopically anomalous C and noble gases. Two morphologic types include grains with smooth or shell-like surfaces and grains that consist of aggregates of smaller particles (*54*). The first class is characterized by particles of well-crystallized graphitic material around a core of more disordered material [randomly oriented graphene layers (*55*)]. The aggregates consist of concentric layers at small scales of poorly graphitized C with turbostratic (*56*) textures. The spherules frequently contain small carbide crystals (5 to 200 nm), ranging in composition from nearly pure TiC to molybdenum and zircon carbides (*57*). Some of these carbides occur in the center of the spherules, pointing to the possibility of heterogeneous nucleation, where the carbides act as condensation nuclei. A model where SiC grains are the condensation nuclei had already been proposed (*58*). However, SiC was not found within the meteoritic presolar carbonaceous material, suggesting that SiC particles form as a separate dust component in stellar outflows.

Evidence for the presence of primitive organic material in the solar system comes from the in situ analysis of carbonaceous chondritic meteorites, interplanetary dust particles (IDPs) of cometary origin collected in the upper atmosphere of Earth, and grains from comet P/Halley (*45*, *59*). The dark matrix of carbonaceous meteorites contains most of the C material in these objects and closely resembles the structure of kerogen (*60*). The meteoritic kerogen-type material can contain a high fraction of PAHs embedded in a system of aliphatic C. Many different organic compounds have been identified in this complicated material (*59*). It is generally assumed that the kerogen-like material formed in the early solar nebula. However, meteoritic kerogen shows a range of D/H abundance enhancements (*61*), which indicates that at least part of the material or its building blocks were formed through gas-phase ion-molecule reactions (*62*) in molecular clouds long before the solar system formed. Cometary IDPs contain a rich distribution of C materials, including PAHs (*63*). Isotopic studies have demonstrated that a large fraction of these grains are also characterized by high D/H ratios (*64*).

Graphite and diamond are the two best-known crystalline structures of C. Fullerite solids are a third type of crystalline C solids (Table 4). Small fullerites (such as C_{60} and C_{70}) are not formed in significant quantities in the low-density and H-rich outflows of C-rich AGB stars and can be excluded as principal IS dust component because of a lack of the characteristic UV double-peak structure in astronomical spectra. A fourth crystalline structure for C solids, carbyne, has also tentatively been proposed (*65*).

Mixed hybridization states lead to curved structures. Examples include fullerites (*41*) and onion-like polyhedral particles where the bending of the graphitic layers is caused by C atoms having tetrahedral bonds (*66*). For carbonaceous solids in the ISM, it is remarkable that irradiation by energetic electrons or ions leads, under appropriate conditions, to the formation of C onions consisting of closed, concentrically arranged and nested, graphitic shells (*67*). Carbon nanotubes are another structure that has attracted much attention in recent years because of their potential wide technological applications (*68*). Nanotubes are cylindrical systems composed of closed

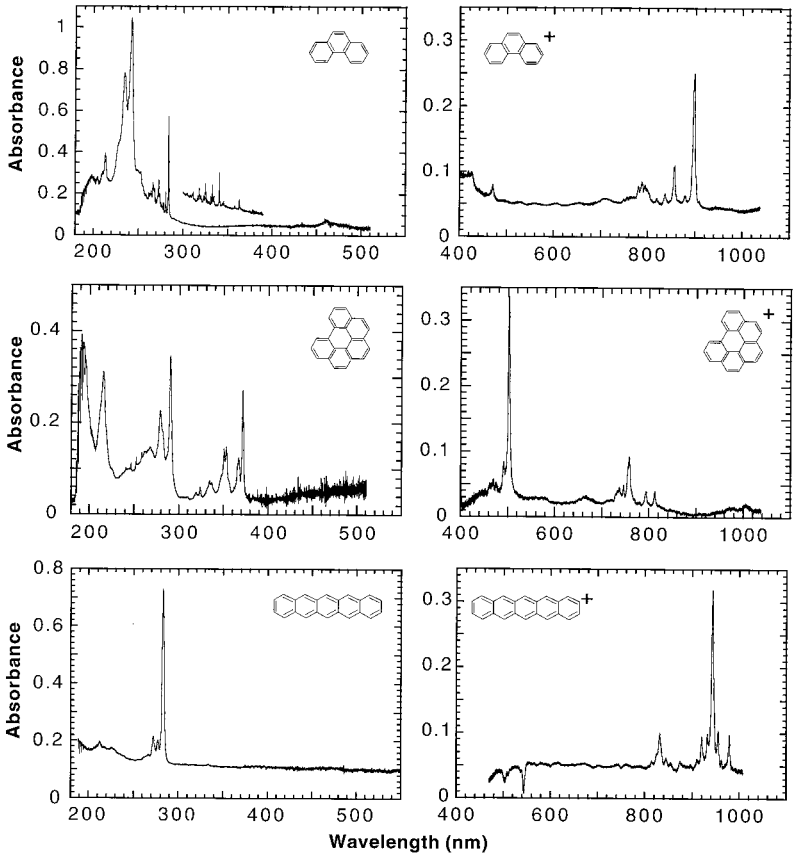

Fig. 2. Electronic spectra of neutral (left) and ionized (right) PAHs isolated at low temperature (5 K) in neon matrices. (From top to bottom) Phenanthrene ($C_{14}H_{10}$), benzo(g,h,i)perylene ($C_{22}H_{12}$), and pentacene ($C_{22}H_{14}$). [Adapted from (*31*)]

Table 3. Spectral signatures attributed to carbonaceous solids.

Feature	Identification
217.5-nm feature	Electronic π-π^* interband transition in H-containing carbonaceous dust
240- to 250-nm feature	Electronic π-π^* interband transition in H-deficient carbonaceous dust
Extended red emission	Luminescence in a-C:H (HAC) particles (excitation by mid-UV photons). Alternative interpretation: Luminescence in other small-particle systems
Plateau emission (6 to 9 μm)	Large hydrocarbon clusters or hydrocarbon nanoparticles
3.4-μm absorption feature with subfeatures	C-H stretching vibrations in aliphatic hydrocarbons

shells capped at each end by pentagons.

Noncrystalline C (Table 4) films and particles are characterized by different sp^2/sp^3 hybridization ratios as well as mixed hybridization states (curved structures) (*69*). Typical structures of C particles are shown in Fig. 3. Each structure critically depends on condensation conditions such as total pressure, temperature, and H or O partial pressures. Hydrogen-rich atmospheres lower the condensation rate and lead preferentially to the production of smaller particles with curved structures (*70*). The resulting materials [for example soot or C black particles, glassy C, or hydrogenated amorphous C films (a-C:H films)] cover a wide range of properties exhibiting different densities, band gap energies, and chemical reactivity (*71*). Therefore, we expect that C grains, forming in the outflows of C-rich AGB stars, cover a wide variety of structures. This is in agreement with astromical observations that point to the formation of noncrystalline C grains with different H contents (*48*).

The astronomically relevant spectral characteristics of C particles in the UV and optical range are dominated by two strong electronic transitions. In general, σ-σ^* interband transitions are centered around 80 nm, whereas π-π^* transitions (present only in graphitic material) are located in a wavelength interval from about 180 to 270 nm. Carbon nanoparticles have a strong tendency to form agglomerates and even to coalesce. This behavior is expected to influence their optical properties, especially at far-infrared (FIR) wavelengths (*72*).

The UV bump at 217.5 nm is the strongest IS extinction feature at optical and UV wavelengths. This feature has been associated with solid C materials or a carbonaceous molecular aggregate, but the precise structure of the carrier is still debated. The main observational constraints concerning the IS UV feature are (*46*) (i) the remarkable constancy of its peak position at 4.60 μm^{-1} (variations $\leq$1%); (ii) the variation of the peak width around a mean value of 1.0 μm^{-1} (variations $\leq$25%); (iii) the lack of correlation between the variations in peak position and width (except for the widest bumps, for which a systematic shift to larger peak wavenumbers is observed in lines of sight passing through dense molecular clouds); (iv) the strength of the feature that requires that an abundant element be part of the carrier material (C, Mg, Si, and Fe); and (v) the fact that no scattering is observed and the feature seems to be produced by pure absorption (Fig. 4).

Small graphite particles were originally proposed to be the band carrier (*46*, *75*). The graphite hypothesis has now been questioned because of its shortcomings, which include the fine-tuning of optical constants and of the particles' size and shape to fit the feature. Furthermore, all models with variations in shape or coating produce correlations between width and peak position, which are not observed.

Theoretical and experimental studies (*71*, *74*, *76*) demonstrate the close relation between the optical properties of carbonaceous grains and their internal structure on length scales ranging from the atomic hybridization state up to the coagulation of nanometer-

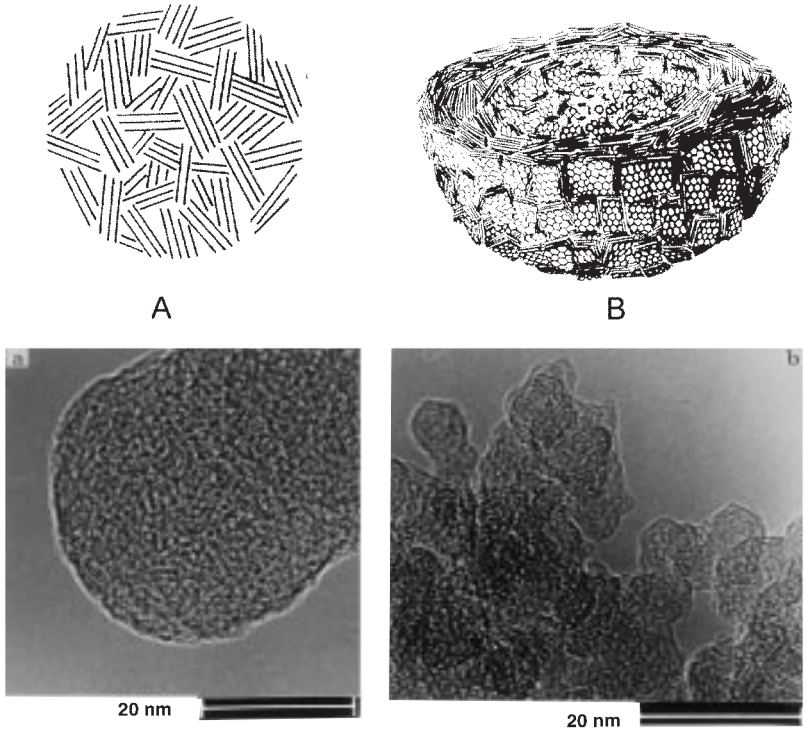

Fig. 3. Two typical structures of C particles taken with a high-resolution transmission electron microscope. (**A**) Carbon particle with randomly oriented basic structural units. (**B**) Onion-type C particle with several condensation seeds.

Table 4. Solid C materials.

Material	Description of structure	Bonding state
Diamond	Tetrahedrally arranged C atoms in a cubic structure	Four sp^3-hybridized orbitals (strong σ bonds with neighboring atoms); electrons completely localized
Graphite	Layers of hexagonally arranged C atoms in a planar condensed ring system (graphene layers); layers are stacked parallel to each other	sp^2 in the layers; weak bonds between layers are metallic (π electrons delocalized over σ skeleton)
Fullerite solids	Geodesic structure of cagelike spheroids; network of 12 five-membered rings (pentagons) and a variable number of six-membered rings (hexagons)	Mixed hybridization state (σ orbitals have partly *p*-orbital character; π orbitals have partly *s*-orbital character)
Carbyne	Long chains with either conjugated triple bonds or cumulated double bonds	*sp* hybridization
Noncrystalline materials	Planar graphitic microcrystallites as "basic structural units" (BSUs) embedded between clusters consisting mostly of sp^3-hybridized C; concentric or random orientation of BSUs possible; formation of bent graphene layers observed: completely amorphous structures with no detectable BSUs also present	Different sp^2/sp^3 ratios; mixed hybridization states

sized particles. For example, a systematic broadening of the π-π^* absorption feature of isolated nanoparticles is correlated with an increased clustering. Small changes in the degree of clustering affect the feature width more strongly than the peak position, which is in accordance with one of the observational constraints. Spectra of isolated nanometer-sized C particles, produced under approriate conditions, show a UV bump as narrow as the IS feature at the right wavelength position (Fig. 4).

The peak position is determined by the internal structure of the individual particles. Recent experiments have shown that the incorporation of H induces a variation in the peak position (*70*, *74*, *77*). On the one hand, H incorporation may be related to smaller crystallite sizes in C grains with disorderly arranged graphitic units. On the other hand, onion-like structures consisting of concentric graphitic units are formed in H-rich atmospheres and have been proposed to be the carrier of the UV bump (*78*). Another suggestion for the carrier is a naphthalene-based molecular aggregate with an aromatic–double ring structure (*79*), which would establish a connection between the UV bump carrier and PAHs.

The spectra of C-rich (and H-rich) AGB stars (the main producers of carbonaceous stardust) show a very weak or no UV bump. These observations imply that the actual band carrier is not present in these environments, and that the carbonaceous solids thought to be produced by C-rich AGB stars must be different from the carriers of the IS extinction bump that are processed by UV irradiation, cosmic rays, and shocks during their residence time of some 10^7 years in the diffuse ISM. However, subjecting small HAC grains to kiloelectron volt He or Ne ions (*80*) leads to a destruction of well-ordered aromatic structures and a weakening of the π-π^* transition. On the other hand, extended irradiation with energetic ions can lead to the production of onion-like particles independent of the precursor material (*81*). As noted above, C onions were proposed to be the carrier of the IS UV feature, although no good laboratory UV spectrum of isolated pure C onions exists. UV irradiation (*82*) of hydrogenated C grains, indeed, activates a UV bump close to the position of the IS feature.

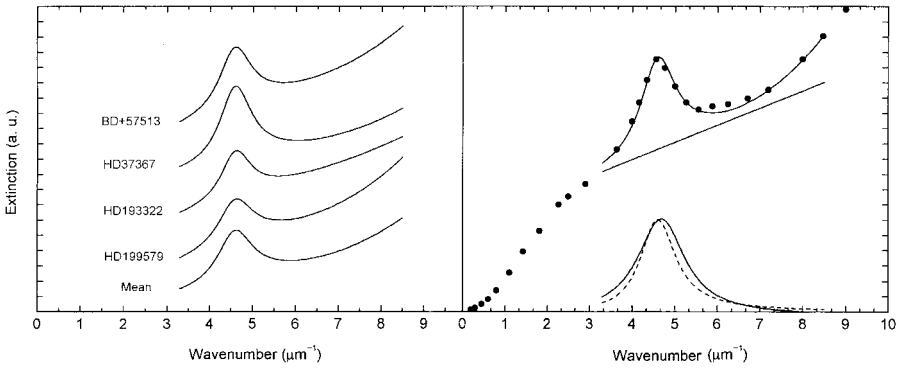

Fig. 4. (**Left**) IS extinction curves toward different stars probing the diffuse ISM and showing the UV feature at 217.5 nm. (**Right**) Upper curves are the mean extinction curve of the diffuse ISM (dots) and its decomposition in a linear background and a Drude profile + far-UV rise. Lower curves show the comparison between the observationally based Drude profile of the mean IS extinction curve (dashed line) and the laboratory spectrum of matrix-isolated nanometer-sized C particles (solid line; corrected for matrix shift). A Drude profile describes the optical behavior of a free-electron conductor. It is here used only as a convenient representation of the UV band profile. [Adapted from (*73*, *74*)]

Table 5. Synopsis of C in space.

Location	Atoms and Molecules	Solids
Carbon-rich circumstellar envelopes around red giants and AGB stars	CO, C_2H_2, complex hydrocarbons, gas-phase PAHs	Non-graphitic C with no pronounced π- π^* transition, silicon carbide
Diffuse ISM	C^+, simple diatomic molecules, gas-phase PAHs and C chains	Graphitic material with strong π-π^* transition, carbonaceous solids with aliphatic hydrocarbons
Dense ISM	CO, complex hydrocarbons	Carbon-containing ices (CO, CO_2, CH_3OH), coagulated carbonaceous grains
IS material in primitive meteorites	PAHs	Carbides, graphitic grains, poorly graphitized C, C onions, nanodiamonds

Conclusion

Carbon in its various forms and structures plays a major role in the evolution of the ISM (Table 5). The widespread distribution of complex organics in the ISM has profound implications for our understanding of the chemical complexity of the ISM, the evolution of prebiotic molecules, and its impact on the origin and the evolution of life on early Earth through the exogenous delivery (by cometary encounters and meteoritic bombardments) of prebiotic organics (*83*). Recent studies of the properties of C materials have generated a wealth of information and have led to the discovery of new forms of C and the development of new techniques in molecular physics.

References and Notes

1. As reported by the Astrochemistry Working Group of Division VI (Interstellar Matter) of the International Astronomical Union (www.strw.leidenuniv.nl/ iau34/links.html).
2. CI is used to denote neutral atomic C (C), CII to denote singly ionized C (C^+), CIII to denote doubly ionized C (C^{2+}), and so forth.
3. The solar mass, $M_\odot$, is equal to 1.989 10^{30} kg.
4. E. M. Burbidge, G. R. Burbidge, W. A. Fowler, F. Hoyle, *Rev. Mod. Phys.* **29**, 547 (1957).
5. $^4He(\alpha,)^8Be(\alpha,)^{12}C^*(,\gamma\ \gamma)^{12}C$.
6. AGB stars have masses $\leq$8 $M_\odot$ and are in a later phase of their evolution, evolving ultimately into planetary nebulae. They are characterized by a very hot core, a high luminosity (3000 $L_\odot$ and higher, with $L_\odot$ = 3.8 10^{26} J s^{-1}), and a surface temperature $<$3000 K. Stars with a higher mass evolve to supernovae of type II. Objects with $\leq$1 $M_\odot$ evolve slowly on the main sequence into White Dwarfs.
7. J. Dorschner and Th. Henning, *Astron. Astrophys. Rev.* **6**, 271 (1995).
8. A. P. Jones and A. G. G. M. Tielens, in *The Cold Universe*, Th. Montmerle, Ch. J. Lada, I. F. Mirabel, J. Trân Thanh Vân, Eds. (Editions Frontiéres, Gif-sur-Yvette, France, 1994), pp. 35–44.
9. Stars with a C/O ratio $>$1 in their stellar mantles and circumstellar envelopes.
10. N. Grevesse and A. Noels, in *Origin and Evolution of the Elements*, N. Prantzos, E. Vangioni-Flam, M. Cassé, Eds. (Cambridge Univ. Press, Cambridge, 1993), pp. 15–25.
11. B stars are stars with a surface temperature in the range 11,000 to 25,000 K. HII regions are regions of ionized atomic hydrogen (H^+) associated with luminous young stars.
12. T. P. Snow and A. N. Witt, *Science* **270**, 1455 (1995).
13. D. M. Meyer, *AIP Conf. Proc.* **402**, 507 (1997); _____, M. Jura, J. A. Cardelli, *Astrophys. J.* **493**, 222 (1998).
14. J. A. Cardelli, D. M. Meyer, M. Jura, B. D. Savage, *Astrophys. J.* **467**, 334 (1996); U. J. Sofia, J. A. Cardelli, K. P. Guerin, D. M. Meyer, *ibid.* **482**, L105 (1997); U. J. Sofia, E. Fitzpatrick, D. M. Meyer, *ibid.* **504**, L47 (1998).
15. The ISM is composed of a number of distinct phases characterized by different physical conditions. The associated gas temperatures and densities span the range from 10 K and $\geq$300 cm^{-3} in molecular clouds, 100 K and 25 to 50 cm^{-3} in diffuse clouds up to 10^4 K and 1 to 10^5 cm^{-3} in HII regions, and 10^6 K and 3×10^{-3} cm^{-3} in the hot intercloud gas [A. G. G. M. Tielens, in *Airborne Astronomy Symposium on the Galactic Ecosystem: From Gas to Stars to Dust*, M. R. Haas, J. A. Davidson, E. F. Erickson, Eds. (Astron. Soc. Pacific Conf. Ser. 73, San Francisco, 1995), pp. 3–22].
16. Charged species govern the coupling of the gas to

magnetic fields and influence the ability of a molecular cloud to collapse and form new stars. The energy and momentum input from stellar radiation and mass loss can lead to the destruction of the parental molecular clouds.
17. PDRs are photon-dominated regions of partially ionized gas around HII regions where stellar photons longward of the Lyman edge dissociate most molecules and ionize atoms with ionization potentials <13.6 eV.
18. D. J. Hollenbach and A. G. G. M. Tielens, *Annu. Rev. Astron. Astrophys.* **35**, 179 (1997).
19. J. G. Ingalls *et al.*, *Astrophys. J.* **479**, 296 (1997).
20. G. Garay, Y. Gomez, S. Lizano, R. L. Brown *ibid.* **501**, 699 (1998).
21. E. J. Korpela, S. Bowyer, J. Edelstein, *ibid.* **495**, 317 (1998).
22. J. Zsargo, S. R. Federman, J. A. Cardelli, *ibid.* **484**, 820 (1997).
23. FUV-to-visible spectroscopy probes the transitions between electronic states. NIR-to-mid-IR spectroscopy probes the transitions within the vibrational manifold of an electronic state. Spectroscopy in the FIR-to-millimeter range probes the rotational transitions of a molecule. Lower energy transitions that result from the coupling between the rotational level and the electronic angular momentum are observed in the microwave range.
24. The sp^j orbitals ($j = 1 - 3$) form the strong σ bond skeleton of the molecule. In the *sp* and sp^2 hybridization states, the remaining *p* electrons, located in a plane normal to the σ bonds, form π bonds, adding to the stability of the molecule.
25. E. F. van Dishoeck, in *The Molecular Astrophysics of Stars and Galaxies*, T. W. Hartquist and D. A. Williams, Eds. (Oxford Univ. Press, Oxford, 1998), pp. 53–99.
26. G. H. Herbig, *Annu. Rev. Astrophys.* **33**, 19 (1995).
27. The main bands fall at 579.9, 585.5, 638.0, and 661.5 nm, respectively [P. J. Sarre, J. R. Miles, S. M. Scarrott, *Science* **269**, 674 (1995)].
28. UIR spectra consist generally of five main bands (3.3, 6.2, 7.7, 8.6, and 11.3 μm) and up to 15 weaker bands, which are not always seen [J. Lequeux, Ed., *Astron. Astrophys.* **315** (1996); T. R. Geballe, in *From Stardust to Planetesimals*, Y. J. Pendleton and A. G. G. M. Tielens, Eds. (Astron. Soc. Pacific Conf. Ser. 122, San Francisco, 1997), pp. 119–127].
29. L. J. Allamandola, A. G. G. M. Tielens, J. R. Barker, *Astrophys. J. Suppl.* **71**, 733 (1989); J. L. Puget and A. Léger, *Annu. Rev. Astron. Astrophys.* **27**, 161 (1989).
30. L. J. Allamandola, D. M. Hudgins, S. A. Sandford, *Astrophys. J.*, in press (1998).
31. F. Salama, in *Low Temperature Molecular Spectroscopy*, R. Fausto, Ed. (Kluwer, Dordrecht, Netherlands, 1996), pp. 169–191.
32. F. Salama, E. Bakes, L. J. Allamandola, A. G. G. M. Tielens, *Astrophys. J.* **458**, 621 (1996).
33. C. Joblin, F. Salama, L. J. Allamandola, in *The Diffuse Interstellar Bands*, A. G. G. M. Tielens and T. P. Snow, Eds. (Kluwer, Dordrecht, Netherlands, 1995), pp. 157–163.
34. In the diffuse ISM, for example, the cold (<100 K), low-density (25 to 30 cm^{-3}), gas is exposed to FUV photons and very energetic cosmic rays.
35. PAHs including heteroatoms (for example, N, O, and S) in their ring structure.
36. I. Cherchneff, in *The Molecular Astrophysics of Stars and Galaxies*, T. W. Hartquist and D. A. Williams, Eds. (Oxford Univ. Press, Oxford, 1998), pp. 265–283.
37. A. Scott, W. W. Duley, G. P. Pinho, *Astrophys. J.* **489**, 193 (1997).
38. Absorption of FUV photons by PAHs leads to the ejection of electrons with excess kinetic energy into the IS gas.
39. P. Thaddeus, *Astrophys. J.* **448**, 545 (1995).
40. Reviewed in F. Salama, in *Solid Interstellar Matter: The ISO Revolution*, A. Jones, C. Joblin, L. d'Hendecourt Eds. (Springer-Verlag, Berlin, 1998), in press.
41. H. W. Kroto, J. R. Heath, S. C. O'Brien, R. F. Curl, R. E. Smalley, *Nature* **318**, 162 (1985).
42. Recent attempts have been successful in measuring the optical spectra of large molecular ions (PAHs) isolated in the gas phase in a supersonic jet expansion under conditions that mimic the IS environment [D. Romanini *et al.*, *Phys. Rev. Lett.*, in press].
43. P. Freivogel, J. Fulara, J. P. Maier, *Astrophys. J.* **431**, L51 (1994).
44. The gas-phase absorption spectrum of C_7^-, recently measured in a supersonic jet expansion, fits a few DIBs [M. Tulej, D. A. Kirkwood, M. Pachkov, J. Maier, *Astrophys. J.* **506**, L69 (1998)].
45. S. A. Sandford, *Meteoritics Planet. Sci.* **31**, 449 (1996); Th. Henning and M. Schnaiter, in *Laboratory Astrophysics and Space Research*, P. Ehrenfreund *et al.*, Eds. (Kluwer, Dordrecht, Netherlands, 1998), in press.
46. E. L. Fitzpatrick and D. Massa, *Astrophys. J.* **307**, 286 (1986); B. T. Draine, in *Interstellar Dust*, *IAU-Symp. 135*, L. J. Allamandola and A. G. G. M. Tielens, Eds. (Kluwer, Dordrecht, Netherlands, 1989), pp. 313–326.
47. J. H. Hecht, *Astrophys. J.* **367**, 635 (1991); J. S. Drilling *et al.*, *ibid.* **476**, 865 (1997).
48. A. Blanco, S. Fonti, V. Orofino, *ibid.* **448**, 339 (1995).
49. D. G. Furton and A. N. Witt, *ibid.* **415**, L51 (1993); K. D. Gordon, A. N. Witt, B. C. Friedmann, *ibid.* **498**, 522 (1998).
50. R. H. Buss Jr. *et al.*, *ibid.* **365**, L23 (1990).
51. Y. J. Pendleton and J. E. Chiar, in *From Stardust to Planetesimals*, Y. J. Pendleton and A. G. G. M. Tielens, Eds. (ASP Conf. Ser. 122, San Francisco, 1997), pp. 179–200.
52. A. K. Speck, M. J. Barlow, C. J. Skinner, *Mon. Not. R. Astron. Soc.* **288**, 431 (1997); R. Papoular, M. Cauchetier, S. Begin, G. LeCaer, *Astron. Astrophys.* **329**, 1035 (1998); H. Muschke, A. C. Andersen, D. Clement, Th. Henning, G. Peiter, *ibid.*, in preparation.
53. E. Anders and E. Zinner, *Meteoritics* **28**, 490 (1993); G. R. Huss and R. S. Lewis, *Geochim. Cosmochim. Acta* **59**, 115 (1995); T. J. Bernatowicz and E. Zinner, Eds., *AIP Conf. Proc.* **402** (1997).
54. E. Zinner, S. Amari, B. Wopenka, R. S. Lewis, *Meteoritics* **30**, 209 (1995).
55. Graphene layers are planar condensed ring systems analogous to a PAH of quasi-infinite size.
56. Structure with graphene layers without a regular stack order.
57. T. J. Bernatowicz *et al.*, *Astrophys. J.* **472**, 760 (1996).
58. M. Frenklach, C. S. Carmer, E. D. Feigelson, *Nature* **339**, 196 (1989); B. J. Cadwell, H. Wang, E. D. Feigelson, M. Frenklach, *Astrophys. J.* **429**, 285 (1994); T. Kozasa, J. Dorschner, Th. Henning, R. Stognienko, *Astron. Astrophys.* **307**, 551 (1996).
59. J. R. Cronin and S. Chang, in *The Chemistry of Life's Origin*, J. M. Greenberg and V. F. Pironello, Eds. (Kluwer, Dordrecht, Netherlands, 1993), pp. 209–258; D. P. Cruikshank, in *From Stardust to Planetesimals*, Y. J. Pendleton and A. G. G. M. Tielens, Eds. (Astron. Soc. Pacific Conf. Ser. 122, San Francisco, 1997), pp. 315–333; M. Mumma, *ibid.*, pp. 369–396.
60. Kerogens are components of terrestrial sedimentary rocks that are insoluble in common organic solvents. They have a cross-linked structure of aliphatic and aromatic hydrocarbons.
61. E. Anders, *Space Sci. Rev.* **56**, 157 (1991).
62. Ion-molecule reactions in molecular clouds lead to fractionation and enlarged D/H ratios in the produced molecules. Other processes such as irradiation of icy grain mantles could also be responsible for the increase of the D/H ratio.
63. S. J. Clemett *et al.*, *Science* **262**, 721 (1993); S. Messenger *et al.*, *Astrophys. J.* **502**, 284 (1998).
64. S. Messenger *et al.*, *Meteoritics* **30**, 546 (1995).
65. R. B. Heimann, *Diamond Relat. Mater.* **3**, 1151 (1994).
66. S. Iijima, *J. Cryst. Growth* **50**, 675 (1980); *J. Phys. Chem.* **91**, 3466 (1987).
67. D. Ugarte, *Nature* **359**, 707 (1992); M. S. Zwanger, F. Banhart, A. Seeger, *J. Cryst. Growth* **163**, 445 (1996).
68. S. Iijima, *Nature* **354**, 56 (1991).
69. J. B. Donnet, *Carbon* **20**, 266 (1982).
70. C. Jäger *et al.*, in preparation.
71. J. Robertson, *Prog. Solid State Chem.* **21**, 199 (1991); R. Papoular *et al.*, *Astron. Astrophys.* **315**, 222 (1996).
72. R. Stognienko, Th. Henning, V. Ossenkopf, *ibid.* **296**, 797 (1995).
73. E. L. Fitzpatrick and D. Massa, *Astrophys. J.* **328**, 734 (1988).
74. M. Schnaiter, H. Mutschke, J. Dorschner, Th. Henning, F. Salama, *ibid.* **498**, 486 (1998).
75. T. P. Stecher and B. Donn, *ibid.* **142**, 1681 (1965).
76. V. Mennella *et al.*, *Astrophys. J. Suppl. Ser.* **100**, 149 (1995); B. Michel, Th. Henning, C. Jäger, U. Kreibig, *Carbon*, in press.
77. V. Mennella *et al.*, *Astrophys. J.* **444**, 288 (1995).
78. W. A. de Heer and D. Ugarte *Chem. Phys. Lett.* **207**, 480 (1993); L. Henrard, A. A. Lucas, Ph. Lambin, *Astrophys. J.* **406**, 92 (1993); L. Henrard, Ph. Lambin, A. A. Lucas *ibid.* **487**, 719 (1997).
79. L. W. Beegle *et al.*, *Astrophys. J.* **487**, 976 (1997).
80. V. Mennella *et al.*, *ibid.* **464**, L191 (1996); Th. Henning, in *Solid Interstellar Matter: The ISO Revolution*, A. Jones, C. Joblin, L. d'Hendecourt, Eds. (Springer-Verlag, Berlin, 1998), in press.
81. P. Wesolowski, Y. Lyutovich, F. Banhart, H. D. Carstanjen, H. Kronmüller, *Appl. Phys. Lett.* **71**, 1948 (1997).
82. V. Mennella *et al.*, *Astrophys. J.* **481**, 545 (1997).
83. F. Salama, *Origins Life Evol. Biosphere* **28**, 249 (1998).
84. We acknowledge the support of the German-American Academic Council through the German-American Research Networking Program. Research on many of the topics covered in this review has been supported by grants from NASA (Office of Space Science, Astrophysics program) to F.S. and by grants from the Deutsche Forschungsgemeinschaft and the Max Planck Society to T.H.